

MC₄: A Hypothetical Three-Dimensional Organometallic Net with Metal–Metal Bonding and Polyacetylene Substructures

Norman Goldberg, Huang Tang, Nancy Kroohs, and Roald Hoffmann*

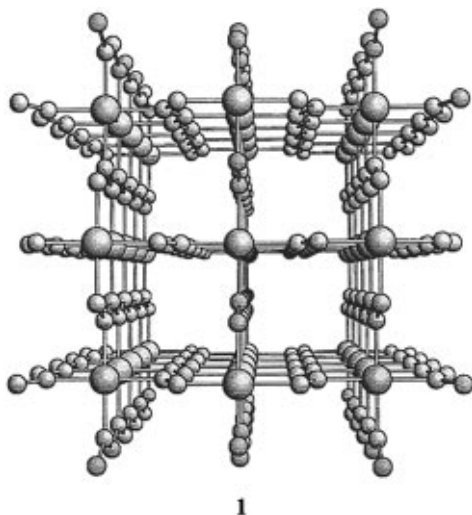
Contribution from the Department of Chemistry and the Materials Science Center
Cornell University, Ithaca, New York 14853-1301

Received June 3, 1996. Revised Manuscript Received August 20, 1996[⊗]

Abstract: The chemical bonding in an intriguing hypothetical organometallic three-dimensional structure, the realization of a (3,4)-connected net, is analyzed by band-structure calculations. The net, stoichiometry FeC₄, has a structure which consists of infinite linear chains of Fe atoms that are cross-linked through kinked polyacetylene-like chains of carbon atoms. Densities of states and calculations (using the extended Hückel approximate molecular orbital method) of a number of related one-dimensional infinite and molecular models are used to describe the bonding characteristics in the carbide. When combined in a three-dimensional framework, carbon and metal chains do not show any tendency to undergo the simple pairing distortions which are characteristic of isolated metal and carbon chains. That these separated chains lose their driving force toward distortion upon fusion is explained by charge transfer from the carbon π -system to the metal d block and a more rigid σ -bonded framework. If one moves to MC₄ with M carrying fewer electrons than Fe, the MM bond strengthens, and CC bonding is weakened; for M having more electrons the trend is reversed. A number of intriguing hypothetical related compounds, formed by incorporation of metal chains into the large channels present in the MC₄ phase or by substitution of polyacenes for polyacetylenes, are proposed.

1. Introduction

Shifting dimensionality and the interplay of organic and inorganic bonding is inherently interesting. In this paper we discuss MC₄ (**1**), a hypothetical three-dimensional structure containing embedded one-dimensional polyacetylene and transition metal chains.¹



1

The geometry of MC₄ is not original to us, but is based on a net described in the beautiful monograph on three-dimensional nets and polyhedra by Wells.^{2,3} The ME₄ net (M = transition metal, E = main-group element) consists of infinite linear chains

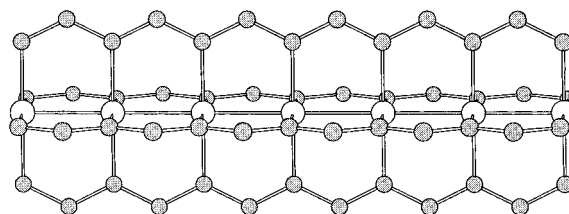
[⊗] Abstract published in *Advance ACS Abstracts*, October 1, 1996.

(1) For a recent review on the chemistry of acetylene–metal complexes, see: Stang, P. J. In *Modern Acetylene Chemistry*; Stang, P. J., Diederich, F., Eds.; VCH Publishers: Weinheim, 1995; and other chapters in this edition.

(2) Wells, A. F. *Three-Dimensional Nets and Polyhedra*; J. Wiley: New York, 1977.

of metal atoms connected to four closest neighbors from four kinked main-group element chains (throughout the paper taken as carbon). The environment of the atoms in the kinked chains is trigonal; that of the M chains can be alternatively described as square planar (so Wells classified this as a (3,4)-connected net), or as distorted octahedral, if the linear M···M contacts come into the bonding region. Several materializations of a (3,4)-connected net are known, such as Ge₃N₄ and the phenacites (Be₂SiO₄).⁴

Does the geometry make sense, for instance for M = Fe and E = C? If we imagine that the kinked chains consist of carbon atoms with a C–C bond distance of 1.40 Å and a C–C–C bond angle of 126° (near the dimensions of polyacetylene), the metal–metal separation that results is a reasonable 2.50 Å. **2** shows a linear chain cut out of the three-dimensional structure and reoriented by 90° relative to **1**.



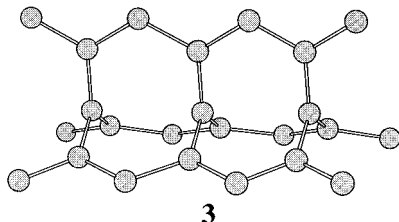
2

Although the three-dimensional interconnected arrangement of such organometallic chains has not yet been observed experimentally, related one-dimensional structures have been characterized. For instance, some main-group elements are known to form similar extended arrangements with trigonal

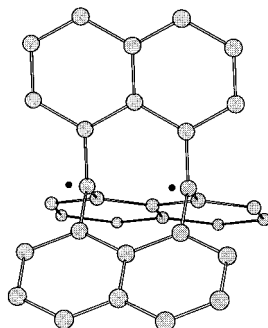
(3) For earlier work on possible new carbon allotropes and on the bonding in (3,4)-connected carbon nets, see: Merz, K. M.; Hoffmann, R.; Balaban, A. T. *J. Am. Chem. Soc.*, **1987**, *109*, 6742.

(4) Greenwood, N. N.; Earnshaw, A. *Chemistry of the Elements*; Pergamon Press: Oxford, 1984.

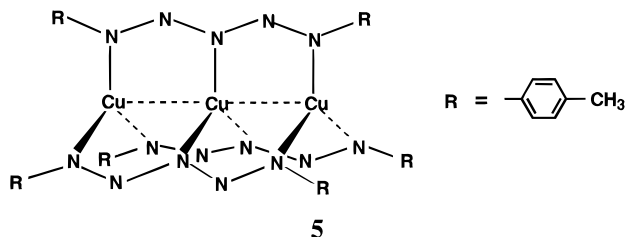
symmetry. Thus, Nesper and co-workers recently observed the structural unit shown in **3** in several silicon-containing Zintl phases.⁵⁻⁷ This $^{\infty}(\text{Si}_7)$ chain consists of three kinked infinite silicon chains which are linked up via centering silicon atoms as indicated. The Si···Si separation along the needle axis is nonbonding, 4.25 Å. A related structure, in this case formed by boron atoms, has been found by Konrad and Jeitschko in the ternary U₅Mo₁₀B₂₄ phase.⁸ Again the central needle B···B contact is very long.

**3**

Some time ago we thought of a chain of type **3**, with carbon atoms. A variant with polyacenes replacing the polyacetylenes is also possible. The nonbonding orbitals of the carbon radicals in the center of the chain would form a half-filled band of substantial width; the expected pairing to form short and long bonds should be inhibited by the strain. To probe this idea, we studied the diradical **4** and its deformation.⁹

**4**

An interesting metal-centered oligomer of type **3** with coppers centering three pentaazenido ligands, **5**, has been reported by Beck and Strähle.¹⁰ Drawing our inspiration from this compound, we also studied the hypothetical infinite systems Cu(N₂)₃ and Cu(N₂)₄, of type **3** and **2**, respectively.¹¹

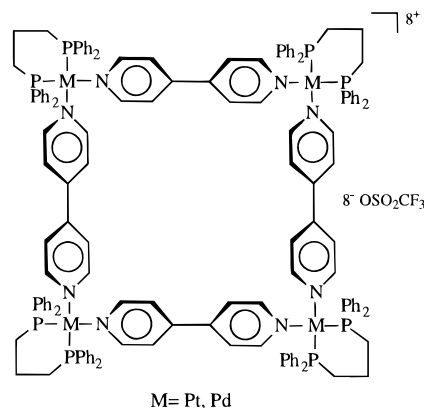
**5**

We should mention that the classical tetraacetate copper

- (5) Nesper, R.; Currao, A.; Wengert, S. In *Organosilicon Chemistry*; Auner, N., Weis, P., Eds.; VCH: Weinheim, 1995, Chapter II.
 (6) Häussermann, C.; Nesper, R. *Angew. Chem., Int. Ed. Engl.* **1995**, *34*, 1462.
 (7) Currao, A.; Wengert, S.; Nesper, R. *Z. Anorg. Allg. Chem.* **1996**, *622*, 501.
 (8) Konrad, T.; Jeitschko, W. *J. All. Comp.* **1996**, *233*, L3.
 (9) Hoffmann, R.; Eisenstein, O.; Balaban, A. *Proc. Natl. Acad. Sci. U.S.A.* **1980**, *77*, 5588.
 (10) Beck, J.; Strähle, J. *Angew. Chem., Int. Ed. Engl.* **1985**, *24*, 409.
 (11) Merz, K. M.; Hoffmann, R. *Inorg. Chem.* **1988**, *27*, 2120.

dimers and many of Cotton's metal-metal multiply bonded molecules¹² can be thought of as dimeric models for the polymer **1**.

And, finally the "square" cavity motif of the MC₄ net, with metal atoms at corners linked by organic spacers, is reminiscent of a fascinating new class of discrete molecular tetranuclear macrocyclic squares prepared by Stang and co-workers.^{13,14} **6** is one example of a number of molecules of this type which are now known.^{1,15,16}

**6**

In this study we use approximate molecular orbital calculations of the tight-binding extended Hückel type¹⁷⁻¹⁹ to investigate the bonding in the hypothetical carbide, FeC₄, as well as some other transition metal phases of the same stoichiometry and related structures. We calculate the band structure and density of states (DOS)^{20,21} for the three-dimensional material, as well as for a number of infinite one-dimensional models which are directly related to the three-dimensional net.

2. Results and Discussion

The hypothetical FeC₄ (**1**) structure has a tetragonal unit cell (space group I4/mmm).² The unit cell contains 4 iron and 16 carbon atoms. In our calculations, the Fe-Fe bond distance is chosen to be 2.50 Å²² and the C-C bond distance is taken as 1.40 Å,²³ corresponding to the average C-C bond distance in polyacetylene.²⁴⁻²⁶ The Fe-C bond distance is fixed at a reasonable 2.00 Å.²⁷

- (12) Cotton, F. A.; Walton, R. A. *Multiple Bonds between Metal Atoms*; Oxford University Press: Oxford, 1993.
 (13) Stang, P. J.; Cao, D. H. *J. Am. Chem. Soc.* **1994**, *116*, 4981.
 (14) Stang, P. J.; Cao, D. H.; Saito, S.; Arif, A. M. *J. Am. Chem. Soc.* **1995**, *117*, 6273.
 (15) Stang, P. J. *Angew. Chem., Int. Ed. Engl.* **1992**, *31*, 274.
 (16) Stang, P. J.; Zhdankin, V. V. *Chem. Rev.* **1996**, *96*, 1123.
 (17) Hoffmann, R. *J. Chem. Phys.* **1963**, *39*, 1397.
 (18) Whangbo, M.-H.; Hoffmann, R. *J. Am. Chem. Soc.* **1978**, *100*, 6093.
 (19) Whangbo, M.-H.; Hoffmann, R.; Woodward, R. B. *Proc. R. Soc. London, Ser. A* **1979**, *366*, 23.
 (20) Hoffmann, R. *Solids and Surfaces: A Chemist's View of Bonding in Extended Structures*; VCH: Weinheim, 1988.
 (21) Burdett, J. K. *Chemical Bonding in Solids*; Oxford University Press: New York, 1995.
 (22) Fehlhammer, W. P.; Stolzenberg, H. In *Comprehensive Organometallic Chemistry*; Wilkinson, G., Ed.; Pergamon Press: Oxford, 1982; Chapter 31.4.
 (23) These choices make the CCC angle a reasonable 126°.
 (24) Hoffmann, R.; Janiak, C.; Kollmar, C. *Macromolecules* **1991**, *24*, 3725 and references therein.
 (25) Yannoni, C. S.; T. C. *Phys. Rev. Lett.* **1983**, *51*, 1191.
 (26) Fincher, C. R.; Chen, C. E.; Heeger, A. J.; MacDiarmid, A. G.; Hastings, J. B. *Phys. Rev. Lett.* **1982**, *48*, 100.
 (27) Orpen, A. G.; Brammer, L.; Allen, F. H.; Kennard, O.; Watson, D. G.; Taylor, R. *J. Chem. Soc., Dalton Trans.* **1989**, S 1.

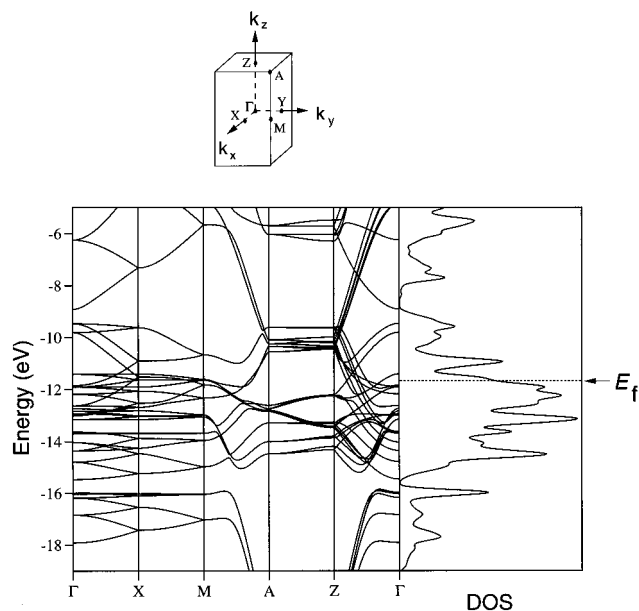


Figure 1. Band structure (left) and DOS (right) of FeC_4 (the dotted line indicates the position of the Fermi level).

The band structure and the total DOS of **1**, calculated by the extended Hückel method,^{18,19} (see Appendix 1 for details), is shown in Figure 1. At first glance the band structure seems to be very complicated; however, one feature of the three-dimensional net suggests a strategy for understanding this complexity: the band dispersion along the z direction is much larger than that along the other directions (compare, for example, the Brillouin zone lines from A to Z with those from M to A or Z to Γ). This, of course, reflects the dominant structural feature of the net—Fe and C chains that align along the z direction; the strongest orbital interactions are also likely to come along this direction. Therefore we deemed it instructive to decompose the structure into separated Fe and C chains, in order to build up an understanding of the electronic features of the three-dimensional system.

Polyacetylene and Linear FeH_4 Chain. Let us quickly recall the bonding in the familiar polyacetylene chain.^{19,24} The band structure of the zigzag *all-trans* $(\text{CH})_\infty$ polymer with equidistant carbons ($\text{CC} = 1.40 \text{ \AA}$) and a CCC angle of 126° is shown in Figure 2a. The bands are labeled as σ or π . The crucial π band is “folded back”^{20,24} at Z, a consequence of the 2_1 screw axis symmetry of the polymer (and the $(\text{CH})_2$ unit cell). The two branches of the π band are labeled π_1 and π_2 . The bonding and antibonding character of the bands can be seen in the crystal orbital overlap population (COOP)^{20,21,28} curves presented in Figure 2c. The top of the π_2 band is C—C π antibonding and the bottom of it is nonbonding; while the top of the π_1 band is nonbonding and the bottom of it is C—C bonding.

It is due to this half-filling of the π band that the symmetric polyacetylene is subject to a Peierls distortion^{19,29} with concomitant opening of a band gap between π_1 and π_2 , and alternating C—C bond distances along the chain. What actually happens upon localization is shown schematically on the right-hand side of Figure 3. The pairing distortion (the two C—C bond lengths we use in our calculations are 1.36 and 1.44 \AA) stabilizes the π_1 band around $k = Z$ and destabilizes π_2 . The driving force to pairing is greatest for a half-filled band, which corresponds to neutral or undoped $(\text{CH})_\infty$. Were we to remove

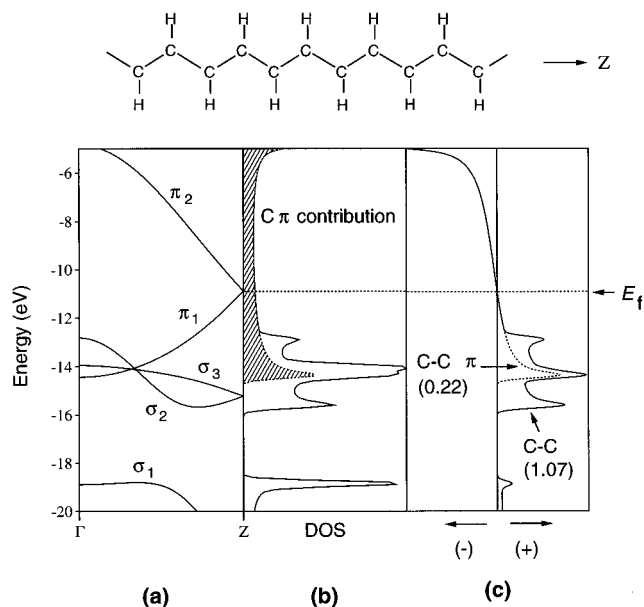


Figure 2. Band structure (a), DOS (b), and COOP (c) of polyacetylene. In part b the solid line corresponds to the total DOS and the shaded area corresponds to the projection of the C π orbitals. In part c the solid line corresponds to the C—C COOP and the dashed line to the C—C π COOP. The numbers indicate the overlap populations for a neutral polyacetylene.

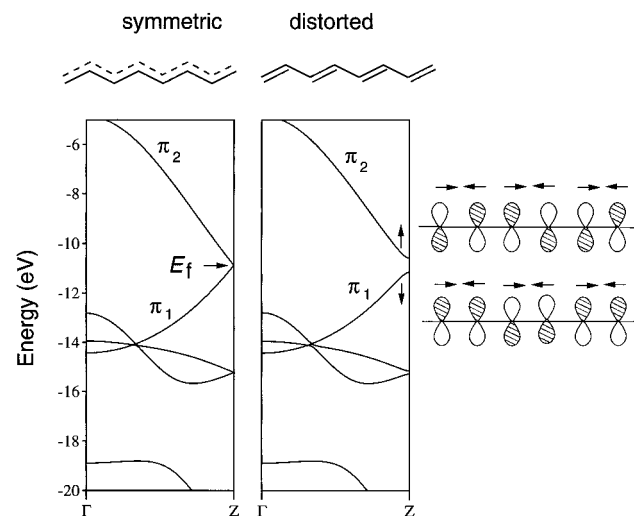


Figure 3. Band structures of undistorted and distorted polyacetylene.

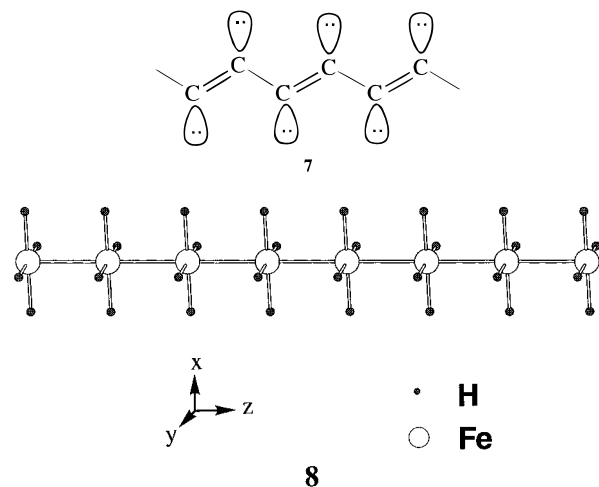
or add electrons to the π band, the simple dimerization would not be as energetically favorable.

The important question for our FeC_4 system is whether or not the Peierls instability of polyacetylene will carry over to the carbon chains in FeC_4 . To address this problem, we need to take a closer look at the interactions between the Fe and C chains and the Fe—Fe interactions in the polymer.

We begin by modeling the Fe chain by itself, substituting all carbon atoms with hydrides. A problem arises at this point—what is the oxidation state of iron? The answer (even granting the formalistic nature of oxidation state assignments) depends on our assumptions concerning the carbon chain ligands. If we assume a resonance structure for each chain as indicated by **7**, it is clear that the carbon chains are $(\text{C}^-)_\infty$, and the oxidation state of Fe in FeC_4 is IV. Hydride (H^-) substitution preserves the local D_{4h} symmetry and the formal oxidation state of the iron in a neutral one-dimensional $(\text{FeH}_4)_\infty$ chain (**8**). The Fe—Fe distance in this model is kept the same as in **1** (2.50 \AA) and the Fe—H distance is chosen to be 1.60 \AA .²⁷

(28) Hughbanks, T.; Hoffmann, R. *J. Am. Chem. Soc.* **1983**, *105*, 3528.

(29) Peierls, R. E. *Quantum Theory of Solids*; Oxford University Press: Oxford, 1972.



The band structure and DOS of **8** (Figure 4) can be readily understood if we begin with the bonding in a monomer, FeH₄, and then build up the polymer. The corresponding interaction diagram for the square-planar FeH₄ molecule is therefore shown at right in Figure 4. Here we observe the familiar four-below-one splitting pattern of the d-block³⁰ in a square-planar ML₄ complex. The positions of the orbitals in the monomer correspond approximately to the centers of the energy bands derived from the band structure calculation of **8**. In Figure 4, the bands are labeled according to their local *D*_{4h} symmetry.

The different dispersion of the d bands results from the different extent of overlap of the five d orbitals with those in the neighboring cells.³¹ The σ band (*a*_{1g}) has the largest dispersion, due to the relatively strong *d*_{z²-*d*_{z² overlap; the top of this σ band is antibonding and the bottom of it is bonding. The degenerate π bands (*e*_g) are flatter because of smaller π overlap between d orbitals. Due to small overlap between δ orbitals, the δ band (*b*_{2g}) is really quite flat. Note that for an electron count of *d*⁴, Fe(IV), there are four electrons to be placed in the four low-lying d bands, making these d bands essentially half-filled.}}

What about dimerization or pairing in (FeH₄)_∞? Is this chain likely to undergo a Peierls distortion like polyacetylene? In Figure 5 left, we prepare for dimerization by doubling the unit cell. At right we show the outcome of the pairing, the band structure of a chain of paired FeH₄ units (alternating Fe–Fe bond lengths of 2.40 and 2.60 Å, respectively). We can see that this pairing distortion, as in the case of polyacetylene, opens up a small band gap at the Fermi level. The σ , π , and δ bands are all split at Z. Upon pairing up two FeH₄ units in (FeH₄)_∞, we observe a decrease in the average energy by 0.3 eV per FeH₄ unit as compared to the symmetric structure. A Peierls pairing distortion is energetically favorable for this one-dimensional chain.

(FeC₈H₄)_∞: A Linear Iron Chain Connected to Four Polyacetylene Chains. As we have seen, an isolated linear chain of iron(IV) ions in a square-planar ligand field should display a tendency for a pairing distortion, just as a single polyacetylene chain does. What happens if we now combine the Fe chain and four polyacetylene chains to form a one-dimensional structure? It is not obvious at all that coupled systems, each individually prone to Peierls distortion, will distort as a whole—witness graphite, just full of polyacetylene-type π -systems, but undeformed.

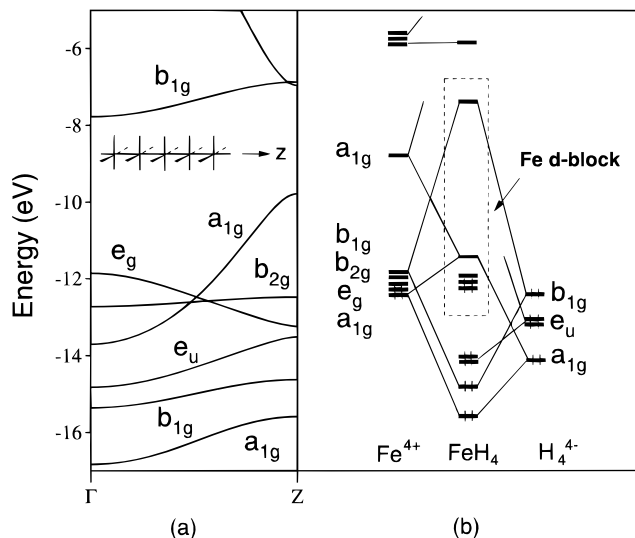


Figure 4. Band structure of (FeH₄)_∞. The FMO diagram of the FeH₄ fragment (right) is shown for comparison.

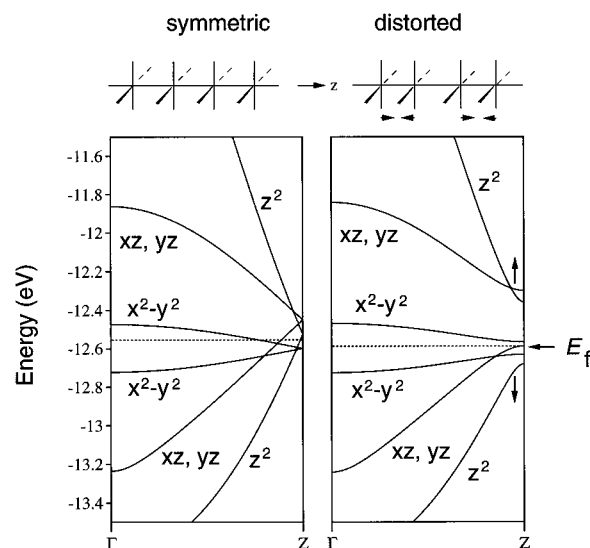
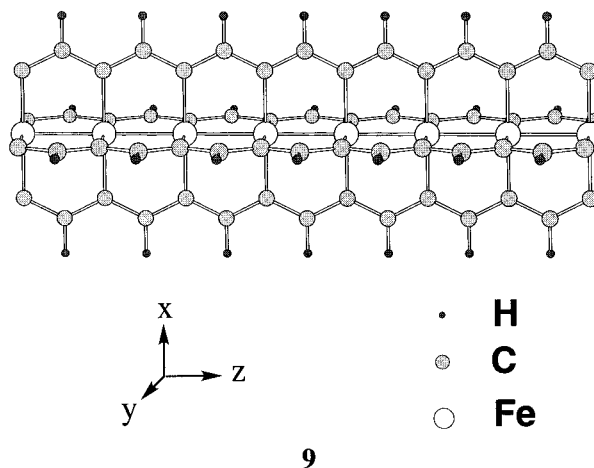


Figure 5. Band structures of a symmetric (left) and paired (right) (FeH₄)_∞ chain.

To approach this question, let us look at the more complicated one-dimensional model, (FeC₈H₄)_∞ (**9**), which is constructed



(30) Albright, T. A.; Burdett, J. K.; Whangbo, M.-H. *Orbital Interactions in Chemistry*; J. Wiley: New York, 1985.

(31) For a discussion of the bonding in related, experimentally known, one-dimensional Pt(CN)₄ chains, see ref 20.

by simply cutting one of the Fe chains and the four surrounding carbon chains out of the three-dimensional FeC₄ net and “passivating” the thus created dangling bonds on every second

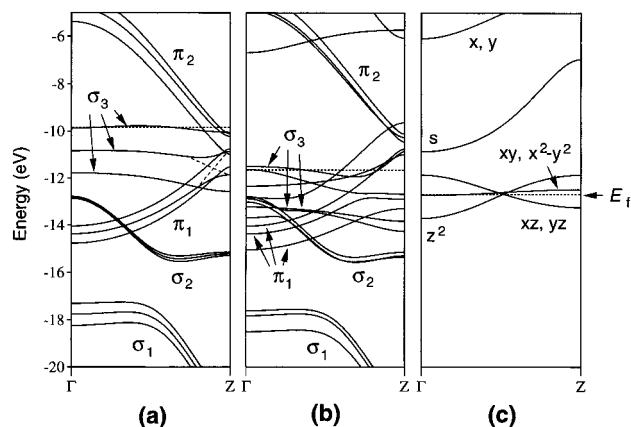
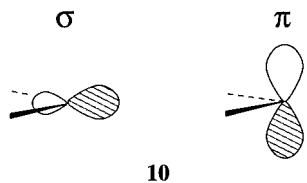


Figure 6. Band structures of four $(\text{C}_2\text{H})_\infty^-$ chains in $(\text{FeC}_8\text{H}_4)_\infty$ (a), a linear chain of Fe^{4+} atoms (c), and $(\text{FeC}_8\text{H}_4)_\infty$ (b). The dotted line marks the Fermi level.

carbon atom by hydrogen atoms (the C–H bond distance is taken as 1.10 Å). In this model there are two types of carbon atoms—one is connected to the iron atoms, the second carbon bridges the former and carries a hydrogen. The bonding in the carbon chain should be quite similar to that in polyacetylene. For those carbon atoms connected to Fe, there are two types of orbitals that are responsible for the Fe–C interactions. One of them, likely to interact more strongly with the iron, is the σ -type orbital illustrated in **10** (left), and the other is a π orbital shown in **10** (right). These orbitals interact with the appropriate symmetry-adapted orbitals on iron.



10

The calculated band structure of this one-dimensional model is shown in Figure 6b. To see how the Fe–C interactions come about we also show the band structure of the sheath, the $(\text{C}_8\text{H}_4^{4-})_\infty$ chain without the central iron atoms (Figure 6a), and that of the inserted linear $(\text{Fe}^{4+})_\infty$ needle (Figure 6c). The bands in Figure 6a have an obvious relationship to those of polyacetylene (see Figure 2a) and are labeled accordingly.

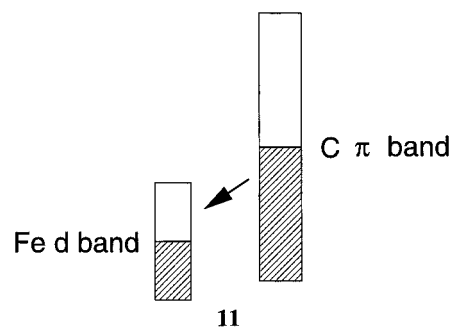
Each polyacetylene chain generates a group of four bands in this model; we seem to see only three because two of them are degenerate in the four-fold symmetry. When the Fe–C interactions are turned off, the band structures (Figure 6a) are very similar to those in polyacetylene, except for the σ_3 bands. These are destabilized because they contain the dangling bonds (the free σ orbitals, as shown in **10**) on every second carbon site. For the linear iron chain (Figure 6c), there are two degenerate δ bands and a low-lying band which is mainly s in character. The relatively narrow d_{z^2} band indicates that the direct Fe–Fe interaction is moderate.

We anticipate substantial interaction, because the iron d orbitals and the polyacetylene σ_3 bands with which they interact are close to each other in energy. Indeed upon inclusion of the iron chain (compare Figures 6c with 6a and 6b) there are considerable changes, which take place mainly in the bands around the Fermi level. One of the $d\delta$ bands ($d_{x^2-y^2}$) is pushed up high in energy as a result of Fe–C σ bonding (it becomes the flat band around -6 eV in Figure 6b). The carbon σ_3 bands are stabilized, a consequence of the Fe–C σ interaction. The Fe σ and δ bands are also substantially rearranged around the zone edge due to their interaction with the carbon σ and π bands.

Much symmetry-allowed mixing takes place between the σ and π bands and we observe a number of avoided crossings. Due to this extensive mixing a strict σ – π separation is no longer possible in the $(\text{FeC}_8\text{H}_4)_\infty$ model. A detailed analysis of the interactions of the π and σ bands is given in the supporting information accompanying this paper.

The calculated average overlap populations (OP) for the $(\text{FeC}_8\text{H}_4)_\infty$ model (**9**) are 0.16 for the Fe–Fe bonds, 0.48 for the Fe–C bonds, and 1.07 for the C–C bonds, respectively. A comparison with the OPs in polyacetylene (OP C–C = 1.08) and $(\text{FeH}_4)_\infty$ (OP Fe–Fe = 0.22) suggests that the C–C bonding in the chain does not change significantly on going from polyacetylene to **9**, while the Fe–Fe bonding is slightly weakened as compared to that in $(\text{FeH}_4)_\infty$. We will return to this point later.

The important qualitative result of our calculations is that the Fermi level of our one-dimensional model now lies *below* the top of the π_1 bands of the polyacetylene sheath. This is a consequence of the energy ordering of the top of the π_1 band and the “center of gravity” of the Fe d bands. Electrons are thus transferred from the polyacetylene π orbitals to the d -block, as shown in **11**. The population analysis also supports this view. In the $(\text{FeC}_8\text{H}_4)_\infty$ model, the population of each carbon π orbital is 0.87 (compared to 1.00 in polyacetylene). The net charge on Fe is -1.03 (compare with $+1.58$ on Fe in $(\text{FeH}_4)_\infty$), while the charge on the C atoms connected to Fe is $+0.05$ and the charge on those not connected to Fe is $+0.14$ (compare with -0.02 on each C in polyacetylene).



11

Note that there is already a band gap between the π_1 and π_2 groups of polyacetylene bands in our model, even though the C–C bond distances are kept the same. This is due to the fact that upon bonding to the Fe chain, the originally degenerate π orbitals of polyacetylene at Z are no longer degenerate; one of the π orbitals interacts with the Fe d_{xy} band, and the other does not.

Will pairing distortion occur in this polymer? We probed several possibilities: dimerization along only the Fe chains; pairing of the polyacetylene chains, and pairing of the Fe chain accompanied by a tetramerization of the polyacetylene chains. None of these distortions opens up a band gap at the Fermi level. We find that all these potential distortions *destabilize* the polymer.

Why does the linear $(\text{FeC}_8\text{H}_4)_\infty$ model not undergo a simple pairing distortion, as polyacetylene does? First of all, both the C π bands and the Fe d bands are no longer half-filled, a consequence of “equalization” of the Fermi level as the component polymers interact. Thus the stabilization upon dimerization in each polymer component, maximal for the half-filled band, is significantly diminished. The second reason is that in general, as a system becomes larger, the driving force for a Peierls distortion is reduced. This is clearly observed, both theoretically and experimentally, when polyacetylene chains are fused to form larger systems such as polyacene and

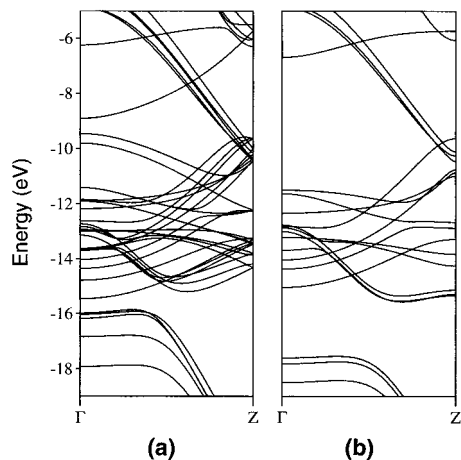


Figure 7. Band structures from Γ to Z of the FeC₄ phase (a) and the one-dimensional model (FeC₈H₄)_∞ (b).

eventually graphite.^{21,32,33} Thus, all the C–C bond distances in a two-dimensional sheet of carbon atoms in hexagonal graphite are identical, despite the fact that the π bands of the polymer are half-filled. Finally, in **9** the repeating unit of the C chain is different from that of the Fe chain. Thus, a pairing distortion of the Fe chain would be associated with a tetramerization along the C chain. The optimum electron counts for distortion in the chains do not match up then. If, on the other hand, we pair up only the C–C bonds along C chains, we do not change the translational symmetry of the Fe chain and therefore we will not observe a band gap opening in the Fe d bands.

In summary, although there is a Peierls instability associated with the separate polyacetylene chain substructures as well as a simple substituted (FeH₄)_∞ chain, when the iron needle and polyacetylene sheath are linked to each other, there is no longer a tendency for a simple dimerization.

Notice that although the Fe–C interactions in our (FeC₈H₄)_∞ model are fairly strong, the carbon chains largely retain the electronic structure of a polyacetylene chain. It is the charge transfer and the structural framework, not the perturbation of the Fe–C bonding, that render a simple distortion mode unlikely.

Bonding in FeC₄. After establishing an understanding of the local bonding in model systems, we are now in a position to discuss the details of the electronic structure of **1**. The first and important point is made by the band structure itself: For three-dimensional FeC₄ (band structure shown in Figure 1) we can see that the behavior of the bands from Γ to Z is very similar to that of (FeC₈H₄)_∞ (Figure 6). The local electronic structure as well as the inter-cell interactions of **1** are directly comparable to that of our one-dimensional model (FeC₈H₄)_∞ (Figure 7).

Let us proceed to discuss the electronic structure of FeC₄ in terms of the densities of states and the contributions of various orbitals to them,^{20,21} in order to obtain more insight into the electronic structure of FeC₄. The DOS of the three-dimensional structure (in **12** we give a slightly different view of the FeC₄ structure) shown in Figure 8 illustrates that the center of most metal d bands lies *below* the Fermi level. In contrast an integration of the C π states shows that they are predominantly (58%) *above* the Fermi level.

If we want to understand the dispersion of the various bands we need to be reminded of the relevant interactions and their magnitudes. The $d_{x^2-y^2}$ orbital on Fe is strongly involved in σ bonding to C while d_{xy} has the right symmetry for π bonding

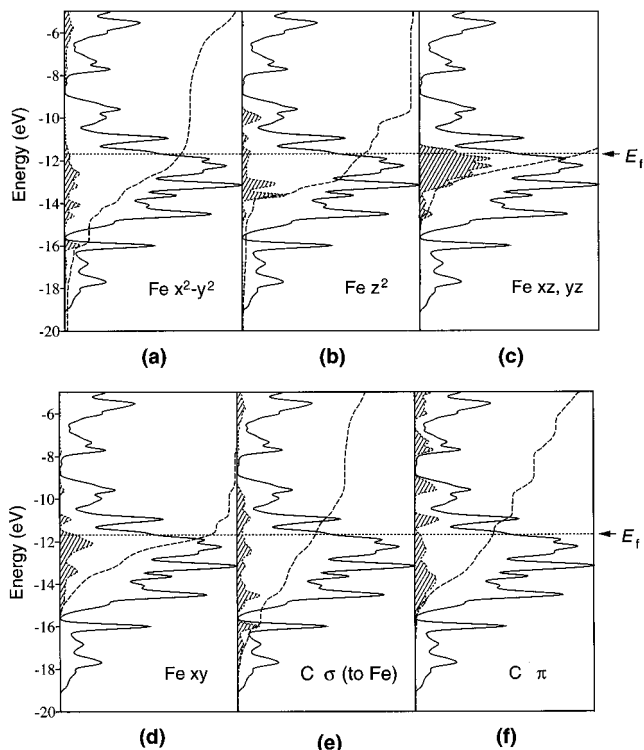
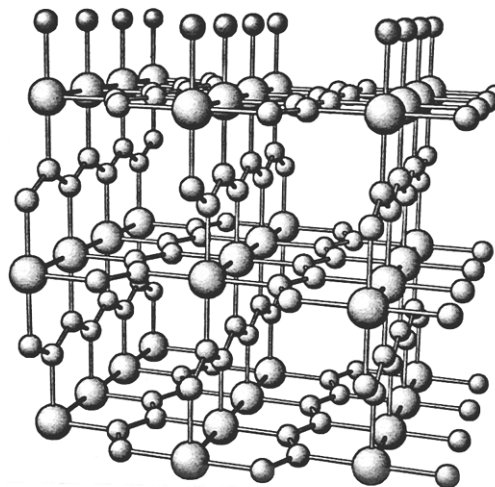
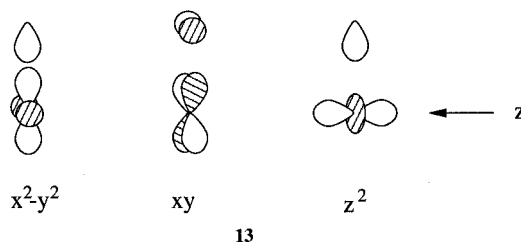


Figure 8. Total DOS of FeC₄ (solid line) and contributions to that DOS (filled areas) of (a) $d_{x^2-y^2}$, (b) d_{z^2} , (c) d_{xz} and d_{yz} , (d) d_{xy} , (e) C σ orbital involved in the Fe–C bonding, and (f) C π orbitals (the dotted lines correspond to the integrations of the individual orbital contributions).



12

(a schematic of the important Fe d-orbital interaction with one carbon center is shown in **13**). The DOS projections of the



13

extended structure show that the Fe $d_{x^2-y^2}$ states indeed are very dispersed, the d_{xy} orbitals less so, due to the Fe–C σ and π

(32) Kertesz, M.; Hoffmann, R. J. *Solid State Chem.* **1984**, *54*, 313.

(33) Burdett, J. K. *Prog. Solid State Chem.* **1984**, *15*, 173.

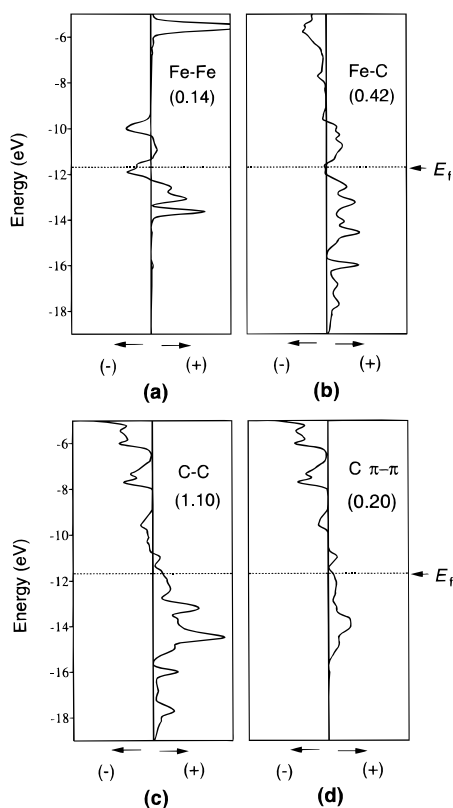


Figure 9. COOP of FeC_4 : (a) Fe–Fe bonding; (b) Fe–C bonding; (c) C–C bonding; and (d) C–C π bonding.

interactions, respectively (compare Figures 8a and 8d). The Fe d_{z^2} band is narrower than $d_{x^2-y^2}$, because the overlap of d_{z^2} with C σ is less. The square-planar ligand field caused by Fe–C bonding is strong. The contribution of $d_{x^2-y^2}$ at high energies is a sign of that (Figure 8a). There is also extensive mixing between the C σ and π bands. This also shows up in the projection of the C σ bands which are responsible for the Fe–C interaction (see Figure 8e). These bands extend to the area above the Fermi level. In polyacetylene there would only be C π states in this region (also see Figure 2). The dispersion of d_{xz} and d_{yz} bands (Figure 8c) is much smaller than those of the $d_{x^2-y^2}$ or d_{z^2} bands, because of the weaker Fe–Fe $d\pi$ interactions. The d_{xy} band (Figure 8d) is broader due to its interaction with the C π bands.

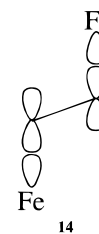
The C π contributions show that the electron population of the originally half-filled polyacetylene π band has been depleted in FeC_4 (the C π band is less than half-filled). We can expect the Fe–Fe bonding to be weaker in FeC_4 than in $(\text{FeH}_4)_\infty$, as the electron transfer leads to a population of Fe–Fe antibonding levels. Similarly, the C–C π interactions should be weakened due to the depopulation of the π bands. The COOP curves (Figure 9) confirm this expectation. Figure 9a shows that Fe–Fe antibonding levels are populated just below the Fermi level. This explains the smaller Fe–Fe OP (0.14) in the three-dimensional net, as compared to that in $(\text{FeH}_4)_\infty$ (0.22). In the COOP plots of the total C–C and C π bonding we see that there is a small portion of the π bonding band above the Fermi level in Figure 9c–d that is left unoccupied. This explains the slightly smaller C–C π OP of 0.20 in FeC_4 as compared with 0.22 in polyacetylene. The electron transfer (C to Fe) is also supported by the calculated average net charges which show that the Fe atom is negatively charged (-0.64) in FeC_4 , while the C atom is positively charged (0.16).

While the C–C π bonding is slightly weakened, the total C–C overlap population (1.10) actually is slightly larger than

Table 1. Average Overlap Populations in FeC_4^q ($q = 4+ \text{ to } 1-$) and CrC_4

| system | overlap populations | | | |
|---------------------|---------------------|------|------|-----------|
| | M–M | M–C | C–C | C–C π |
| FeC_4^{4+} | 0.17 | 0.41 | 1.05 | 0.17 |
| FeC_4^{3+} | 0.18 | 0.42 | 1.06 | 0.18 |
| FeC_4^{2+} | 0.17 | 0.42 | 1.08 | 0.19 |
| FeC_4^{1+} | 0.15 | 0.42 | 1.09 | 0.19 |
| FeC_4^0 | 0.14 | 0.42 | 1.10 | 0.20 |
| FeC_4^{1-} | 0.12 | 0.42 | 1.11 | 0.20 |
| CrC_4 | 0.28 | 0.53 | 1.09 | 0.19 |

that (1.07) of polyacetylene. This suggests that the C–C σ bonding is stronger in FeC_4 than in polyacetylene. As **14** shows, the Fe–C σ -bonding orbitals are also of the right symmetry to be involved in CC bonding (part σ , part π). It appears that if the Fe–C bond in FeC_4 is weaker than C–H in polyacetylene, there is some compensation in the C–C bond.



14

The important question we have asked before is whether FeC_4 might possibly undergo a distortion to a less symmetric structure. Despite substantial investment of effort in exploring this, we do not find a mode that stabilizes the system via opening of a band gap at the Fermi level. Neither a pairing distortion nor a linearization of the kinked carbon chains is energetically favorable according to our calculations. Similar effects to those responsible for the stability of the symmetrical one-dimensional model $(\text{FeC}_8\text{H}_4)_\infty$ are at work; most importantly, there is a strong electron transfer from the carbon π to the Fe d levels. The stronger σ framework of the carbon chains that we find also contributes, we think, to the stability of the distorted form.

The FeC_4 structure we calculate should be metallic. The structure has obvious anisotropies in it, which may give rise to interesting electronic properties, should it ever be made. And the localization modes we worried about may emerge as charge density waves.²¹

MC₄ Phases with Other Transition Metals. The population of Fe–Fe antibonding levels in FeC_4 makes one wonder whether it might be possible to achieve a more stable system with different first-row transition metals. A direct comparison of the OP's (tentatively taken as a sign of bond strength) for different transition metals is problematic within extended Hückel theory. However, we can model the behavior of different metals by varying the overall charge of the FeC_4^q phase. The calculated overlap populations for FeC_4^q ($-1 \leq q \leq 4$) and those of the corresponding CrC_4 system (same geometry as FeC_4) are shown in Table 1.

As expected from the nature of the bands around the Fermi level (Figure 9 is our guide here), the trends for C–C and Fe–Fe bonding are opposite. The average OP for the Fe–Fe interaction decreases slightly upon addition of more electrons, while the C–C σ and π OP actually becomes larger. Upon decreasing slightly the numbers of electrons (from FeC_4) antibonding metal d levels are depopulated and thus the M–M OP increases; C–C bonding states are less occupied, so this bond weakens. The iron–carbon OP is not really affected. Most of the significant C–Fe σ bonding bands lie below the region

of the Fermi level. It seems to us (we have no real justification for this supposition) that in these systems it is important to have as much metal–metal bonding as possible, so that we suggest lower electron counts are the direction to go.

The table also includes a calculation on CrC₄; the overlap populations are shown in Table 1. For calibration, we constructed a Cr–Cr singly bonded system (Cr₂(CO)₁₀²⁻) and a quadruply bonded Cr₂(CH₃)₈⁴⁻ (both with M–M distance of 2.50 Å). The calculated OP's for the singly bonded carbonyl complex (Cr–Cr OP = 0.23) and the quadruply bonded one (Cr–Cr OP = 0.43) show that the metal–metal bond in the hypothetical CrC₄ phase (Cr–Cr OP = 0.28) would be slightly stronger than a normal Cr–Cr single bond.

We also studied the pairing distortion with other metals. As in the case of (FeC₈H₄)_∞, we do not find any simple deformation mode that opens up a band gap at the Fermi level and stabilizes these transition metal systems.

3. Concluding Remarks

We have analyzed the bonding in FeC₄, a hypothetical three-dimensional structure consisting of coupled infinite chains of Fe with C in a polyacetylene substructure. Comparison of the structural and bonding features of a number of related models of lower dimensionality has been used to understand the three-dimensional system. Our calculations indicate that the Peierls distortions indicated by the electronics of the one-dimensional carbon and FeH₄ chains are not likely to occur in the three-dimensional system. Here charge transfer from the carbon chains to the d-bands of iron and the more extensive σ framework in the three-dimensional structure render such distortions energetically unfavorable.

Our investigation of the bonding in FeC₄ suggests that this three-dimensional structure could be an interesting synthetic target. It is possible in principle to either increase M–M bonding (with some loss of C–C bond strength) by decreasing the electron count or increase the C–C bonding (with some loss of metal bond strength). So different metals might be tried. Since there are some parts of the C–C bonding bands which are unfilled, there is a possibility that compounds with even higher electron counts might also be stable, though this would occur at the expense of metal–metal bonding.

How might such systems as we have calculated be made? One-dimensional linear carbon chains can be synthesized^{34,35} and we think it would be intriguing to see if these chains can be combined with metal atoms to form three-dimensional nets such as FeC₄. In the Fe–C and Cr–C systems so far there are very few carbon-rich phases known.^{36–40} Although some mixed phases with a higher carbon content, such as LnFeC₄,^{41–43} LnFeC₂⁴¹ have been characterized, disproportionation to graphite and/or stable phases such as cementite (Fe₃C) will be a real thermodynamic problem.

(34) Man, L. I.; Malinovskii, Y. A.; Semiletov, S. A. *Sov. Phys. Cryst.* **1990**, *35*, 608.

(35) Lagow, R. L.; Kampana, J. J.; Wei, H.-C.; Battle, S. L.; Genge, J. W.; Laude, D. A.; Harper, C. J.; Bau, R.; Stevens, R. C.; Haw, J. F.; Munson, E. *Science* **1995**, *267*, 362.

(36) A nice compilation of the structural and electronic properties of transition metal carbides is given in: Cottrell, A. *Chemical Bonding in Transition Metal Carbides*; The Institute of Materials: London, 1995.

(37) Fasika, E. J.; Jeffrey, G. A. *Acta Crystallogr.* **1965**, *19*, 463.

(38) Caer, G. I.; Dubois, J. M.; Senteur, J. P. *J. Solid State Chem.* **1976**, *19*, 19.

(39) Yakel, H. L., *Int. Metals Rev.* **1985**, *30*, 17.

(40) Dyson, D. J.; Andrews, K. W. *J. Iron Steel Inst.* **1969**, *207*, 208.

(41) Marusin, E. P.; Bodak, O. I.; Tsokol', A. O.; Baivel'man, M. G. *Sov. Phys. Crystallogr.* **1985**, *30*, 340.

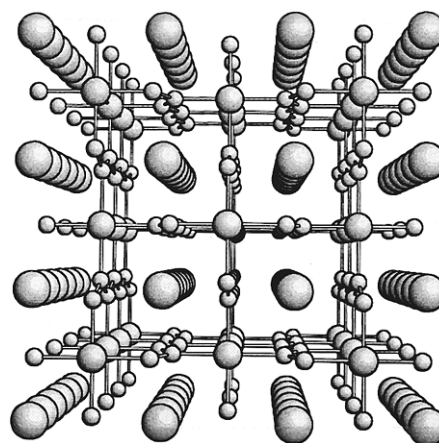
(42) The geometry of this FePtC₄ phase is such that the atoms within each Pt needle are "facing" the centers of C–C bonds in the carbon chains.

Table 2. Atomic Parameters Used in the Extended Hückel Calculations

| atom | orbital | H_{ii} | ζ_1 | c_1^a | ζ_2 | c_1^a | ref |
|------|---------|----------|-----------|---------|-----------|---------|-----|
| C | 2s | -21.40 | 1.625 | | | | 17 |
| | 2p | -11.40 | 1.625 | | | | |
| H | 1s | -13.60 | 1.30 | | | | 17 |
| | Cr | 4s | -8.66 | 1.70 | | | 48 |
| | | 4p | -5.24 | 1.70 | | | |
| Fe | 3d | -11.22 | 4.95 | 0.5058 | 1.80 | 0.6747 | 48 |
| | 4s | -9.10 | 1.90 | | | | |
| | 4p | -5.32 | 1.90 | | | | |
| | 3d | -12.60 | 5.35 | 0.5505 | 2.00 | 0.6260 | |
| Pt | 6s | -9.077 | 2.55 | | | | 48 |
| | 6p | -5.475 | 2.55 | | | | |
| | 5d | -12.59 | 6.013 | 0.6334 | 2.696 | 0.5513 | |

^a Coefficients in double- ζ expansion.

It might be possible, though, to stabilize the system by incorporation of other metal chains in the channels present in the MC₄ structure. The perpendicular distance between the plane of one polyacetylene-like carbon chain and the next is quite large (4.7 Å); if one were to insert another metal needle in the square channels, M'MC₄ (**15**), one would have a π -bonding M–C distance of 2.45 Å.⁴² This is a little long, for the η^2 -C₂–Pt distance in acetylene complexes is known to lie around 2.03 Å.²⁷

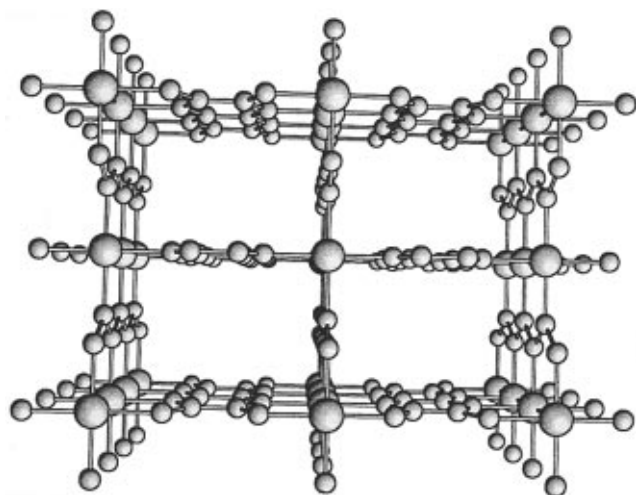


15

We have calculated such an M'MC₄ phase with Pt chains in the channels.⁴⁴ The OPs for this FePtC₄ phase (Fe–Fe = 0.14, Fe–C = 0.42, C–C 1.05, C π –C π = 0.14, C–Pt = 0.02 and Pt–Pt = 0.16) show that the C–C π -bonding interaction is slightly weaker in this compound; the Pt–C π bond is not very strong either due to the relatively long Pt–C distance. It might nevertheless be possible that such a phase slightly adjusts its geometry to enable better overlap between the Pt needles and the carbon chains. We have not yet attempted to model this possible distortion. What if the carbon subsystem is made larger? One could think of replacing the kinked carbon chains by larger carbon substructures such as polyacene. The calculated band structure for this FeC₈ phase is rather similar to that of FeC₄. The channels are now much bigger; the perpendicular distance between the polyacenes is 6.1 Å and one might be able to incorporate larger element or metal substructures into such a phase. Finally one can generate (on paper, where synthesis is easy) a mixed polyacetylene, polyacene system with rectangular

(43) σ bonded acetylene–Pt complexes are well-known. See for example: Markwell, R. D.; Butler, I. S.; Kakkar, A. K.; Kahn, M. S.; Al-Zakwani, Z. H.; Lewis, J. *Organometallics* **1996**, *15*, 2331 and references therein.

channels (16). Theoretically, this should also be metallic.



16

Acknowledgment. Thanks are due to Greg Landrum, Hugh Genin, and Stephen Lee for helpful discussions. N. G. is grateful to the Deutsche Forschungsgemeinschaft (DFG) for a research fellowship. We are indebted to the National Science

Foundation for supporting our work through Research Grant CHE-9408455.

Appendix 1

The calculations presented in this work have been carried out in the framework of the extended Hückel tight-binding method^{18,19} using the marvelous YAeHMOP package.⁴⁴ The parameters used in the calculations are listed in Table 2. The off-diagonal elements of the Hamiltonian were evaluated with the modified Wolfsberg–Helmholtz formula.⁴⁵ Numerical integrations over the symmetry-unique section of the Brillouin zone of the three-dimensional material were performed using a 40 k-point set obtained by the method of Ramirez and Böhm.^{46,47} For the one-dimensional chains a 60 k-point set was used.

Supporting Information Available: A detailed analysis of the orbital mixing in $\text{Fe}(\text{C}_3\text{H}_4)$ (3 pages). See any current masthead page for ordering and Internet access instructions.

JA961868L

(44) The great YAeHMOP package is freely available on the WWW at: <http://overlap.chem.cornell.edu:8080/yaehmop.html> Landrum, G. A. (1995).

(45) Ammeter, J. H.; Bürgi, H.-B.; Thibault, J. C.; Hoffmann, R. *J. Am. Chem. Soc.* **1978**, *100*, 3686.

(46) Ramirez, R.; Böhm, M. C. *Int. J. Quantum Chem.* **1986**, *30*, 391.

(47) Ramirez, R.; Böhm, M. C. *Int. J. Quant. Chem.* **1988**, *34*, 571.

(48) Summerville, R. H.; Hoffmann, R. *J. Am. Chem. Soc.* **1976**, *98*, 7240.